


Induction of aryl hydrocarbon receptor in granulosa cells by endoplasmic reticulum stress contributes to pathology of polycystic ovary syndrome

Chisato Kunitomi, Miyuki Harada *, Akari Kusamoto, Jerilee Mk Azhary, Emi Nose, Hiroshi Koike, Zixin Xu, Yoko Urata, Nozomi Takahashi, Osamu Wada-Hiraike, Yasushi Hirota , Kaori Koga, Tomoyuki Fujii, and Yutaka Osuga

Department of Obstetrics and Gynecology, Faculty of Medicine, The University of Tokyo, Bunkyo, Tokyo 113-8655, Japan

*Correspondence address. Department of Obstetrics and Gynecology, Faculty of Medicine, The University of Tokyo, 7-3-1, Hongo, Bunkyo, Tokyo 113-8655, Japan. Tel: +81-3-3815-5411; Fax: +81-3-3816-2017; E-mail: haradam-ky@umin.ac.jp  <http://orcid.org/0000-0003-1071-5600>

Submitted on November 08, 2020; resubmitted on January 04, 2021; editorial decision on January 15, 2021

ABSTRACT: Recent studies have uncovered the critical role of aryl hydrocarbon receptor (AHR) in various diseases, including obesity and cancer progression, independent of its previously identified role as a receptor for endocrine-disrupting chemicals (EDCs). We previously showed that endoplasmic reticulum (ER) stress, a newly recognized local factor in the follicular microenvironment, is activated in granulosa cells from patients with polycystic ovary syndrome (PCOS) and a mouse model of the disease. By affecting diverse functions of granulosa cells, ER stress contributes to PCOS pathology. We hypothesized that expression of AHR and activation of its downstream signaling were upregulated by ER stress in granulosa cells, irrespective of the presence of EDCs, thereby promoting PCOS pathogenesis. In this study, we found that AHR, AHR nuclear translocator (ARNT), and AHR target gene cytochrome P450 1B1 (CYP1B1) were upregulated in the granulosa cells of PCOS patients and model mice. We examined CYP1B1 as a representative AHR target gene. AHR and ARNT were upregulated by ER stress in human granulosa-lutein cells (GLCs), resulting in an increase in the expression and activity of CYP1B1. Administration of the AHR antagonist CH223191 to PCOS mice restored estrous cycling and decreased the number of atretic antral follicles, concomitant with downregulation of AHR and CYP1B1 in granulosa cells. Taken together, our findings indicate that AHR activated by ER stress in the follicular microenvironment contributes to PCOS pathology, and that AHR represents a novel therapeutic target for PCOS.

Key words: aryl hydrocarbon receptor / cytochrome P450 1B1 / endoplasmic reticulum stress / granulosa cell / polycystic ovary syndrome

Introduction

Polycystic ovary syndrome (PCOS) is the most common endocrine and metabolic disorder in women of reproductive age, affecting 6–20% of women in this age group; however, its pathophysiology remains to be fully elucidated (Escobar-Morreale, 2018). Recent studies have uncovered that the aryl hydrocarbon receptor (AHR), a well-established receptor for endocrine-disrupting chemicals (EDCs), controls the expression of a diverse set of genes, and thus plays an important role in cellular homeostasis and disease, including various metabolic,

developmental, and pathologic processes, independently of its activity as an EDC receptor (Pocar *et al.*, 2005; Swedenborg *et al.*, 2009; Esser *et al.*, 2018). Moreover, expression of AHR and activation of its downstream signaling are regulated by a variety of stimuli, including growth factors and hormones, in the absence of its ligands (Harper *et al.*, 2006; Larigot *et al.*, 2018). Hence, in this study, we focused on the role of AHR in PCOS pathophysiology irrespective of the presence of EDCs.

Endoplasmic reticulum (ER) stress is a newly recognized local factor in the follicular microenvironment. ER stress involves the accumulation

of unfolded or misfolded proteins in the ER and is the consequence of various physiological and pathological conditions that increase the demand for protein folding or attenuate the protein-folding capacity of the ER. ER stress results in activation of several signal transduction cascades, collectively termed the unfolded protein response (UPR), which affect a wide range of cellular functions (Rutkowski and Kaufmann, 2007; Walter and Ron, 2011; Hetz et al., 2020). Previously, we showed that ER stress is activated in granulosa cells from PCOS patients and a mouse model of the disease, and that it affects diverse cellular functions of granulosa cells, including production of profibrotic growth factors, induction of apoptosis, and accumulation of advanced glycation end products (AGEs), thereby contributing to PCOS pathology (Takahashi et al., 2017a; Azhary et al., 2019, 2020).

On the basis of these findings, we hypothesized that expression of AHR and activation of its downstream signaling are upregulated by ER stress in granulosa cells and contribute to PCOS pathology, irrespective of the presence of EDCs. To test this hypothesis, we measured the expression of AHR, AHR nuclear translocator (ARNT), and cytochrome P450 1B1 (CYP1B1) in granulosa cells of PCOS patients and mice with dehydroepiandrosterone (DHEA)-induced PCOS. To evaluate the activation of AHR downstream signaling, we selected CYP1B1 as a representative AHR target gene; CYP1B1 is a well-established xenobiotic enzyme whose expression is correlated with AHR activity (Hao et al., 2012; Stockinger et al., 2014). We then determined the effects of ER stress on expression of AHR, ARNT, and CYP1B1, and the intermediary role of AHR in activating CYP1B1 in cultured human granulosa-lutein cells (GLCs). We also determined the *in vivo* effects of an AHR antagonist on estrous cycle and atretic antral follicle formation, as well as expression of AHR and CYP1B1 in granulosa cells in a mouse model of PCOS.

Materials and methods

Human specimens

GLCs were obtained from patients undergoing oocyte retrieval for IVF at the University of Tokyo Hospital, Matsumoto Ladies Clinic, Hamada Hospital, Akihabara ART Clinic, and Phoenix ART Clinic. For comparison of mRNA levels of *AHR*, *ARNT*, and *CYP1B1* in GLCs, 12 control patients and 12 patients with PCOS were examined. There were no significant differences between the groups in terms of age, BMI, serum basal FSH level, and controlled ovarian stimulation (COS) (Table 1). However, LH level, the LH/FSH ratio, and anti-Müllerian hormone (AMH) level were significantly higher in PCOS patients, as expected. The number of oocytes retrieved was smaller in PCOS group, which may be attributable to clinicians' preference to milder stimulation with significantly lower total dose of FSH for PCOS patients. Women with PCOS were diagnosed according to the Rotterdam criteria (Rotterdam ESHRE/ASRM-Sponsored PCOS Consensus Workshop Group, 2004). The inclusion criteria for the control group were a normal ovulatory cycle, no endocrine abnormalities, and a normal ovarian morphology as determined by ultrasound. For immunohistochemical analysis, ovaries were collected from five control patients and five patients with PCOS. For control samples, normal ovaries were obtained from women with regular menstrual cycles without hormonal treatment who underwent radical or extended hysterectomy for

carcinoma of the uterine cervix or endometrium. PCOS ovaries were obtained from women with oligo- or amenorrhea who also underwent radical or extended hysterectomy for carcinoma of the uterine cervix or endometrium. The findings of polycystic ovaries were histologically confirmed. There was no significant difference in age between the groups, whereas BMI was significantly higher in PCOS patients: age was 32.0 (27–46) (median, range) versus 27.0 (24–36) years old (control versus PCOS, $P=0.1944$); and BMI was 18.99 (16.33–20.96) versus 28.75 (25.97–31.96) kg/m^2 (control versus PCOS, $P=0.0003$). Ovaries were sectioned at 5 μm before being subjected to staining, and at least three sections from each sample were analyzed. All experimental procedures were approved by the relevant institutional review boards (authorization reference number: 3594-6). All patients provided signed informed consent, and the study was conducted in accordance with the principles of the Declaration of Helsinki.

Animal model

A well-established DHEA-induced PCOS mouse model was used in this study (Ela et al., 2006; Lai et al., 2014; Takahashi et al., 2017a). Three-week-old female BALB/c mice were obtained from Japan SLC (Hamamatsu, Japan). The animals were divided into three groups: control, PCOS, and PCOS plus CH223191 (an AHR antagonist). The control group ($n=7$) was injected s.c. with sesame oil every day for 20 days. The PCOS group ($n=7$) received daily s.c. injection with DHEA (6 mg/100 g body weight; Sigma-Aldrich, St. Louis, MO, USA) for 20 days. Mice in the PCOS plus CH223191 group ($n=7$) received daily s.c. injection of DHEA for 20 days and s.c. injection of CH223191 (10 mg/kg body weight; Selleck, Houston, TX, USA) from day 8 to 20. Ovaries were collected on day 21. The procedures and dose of CH223191 were determined as previously described (Dean et al., 2018; Wang et al., 2018). All procedures described in this study were approved by the University of Tokyo Committee on the Use and Care of Animals and were performed in accordance with relevant guidelines and regulations.

Immunohistochemistry

Human and mouse ovarian sections were immunostained with anti-AHR (RRID: AB_2226163, 1:50; Proteintech Group, Tokyo, Japan), anti-ARNT (RRID: AB_10639523, 1:600; Proteintech), and anti-CYP1B1 antibodies (RRID: AB_731810, 1:1500; Abcam, Cambridge, UK). Isotype-specific IgG served as a negative control. Antigen retrieval was performed using target retrieval solution (Dako, Tokyo, Japan). Immunohistochemistry was performed at least five times independently using identical samples. The ImageJ software (RRID:SCR_003073; National Institutes of Health, Bethesda, MD, USA) was used for quantitative analysis (Schneider et al., 2012). Positively stained granulosa cells were counted in six randomly selected follicles from five individual patients or mice.

Isolation and culture of human GLCs

GLCs obtained from women without PCOS were used for cultures. Isolation of GLCs was performed as reported previously (Takahashi et al., 2019; Azhary et al., 2020; Kunitomi et al., 2020). Briefly, follicular fluids were centrifuged and resuspended in phosphate-buffered saline (PBS) with 0.2% w/v hyaluronidase (Sigma-Aldrich) and incubated at

Table 1 Characteristics of the patients who provided follicular fluid samples.

| | Control (n = 12) | PCOS (n = 12) | P-value |
|-------------------------------------|---------------------|---------------------|---------|
| Age (years) | 36.0 (31–41) | 34.0 (29–40) | 0.1207 |
| BMI (kg/m ²) | 22.16 (19.71–28.38) | 23.30 (18.08–32.47) | 0.3824 |
| LH (mIU/mL) | 4.4 (2.1–6.3) | 7.7 (1.7–15.4) | 0.0017* |
| FSH (mIU/mL) | 7.75 (6.0–15.4) | 6.85 (4.9–9.6) | 0.2173 |
| LH/FSH | 0.60 (0.23–0.78) | 1.27 (0.19–2.23) | 0.0003* |
| Anti-Müllerian hormone (ng/mL) | 2.555 (0.46–7.66) | 8.135 (2.32–24.63) | 0.0077* |
| Controlled ovarian stimulation (n): | | | 0.6091 |
| Antagonist | 6 | 6 | |
| FSH | 3 | 5 | |
| Long | 2 | 0 | |
| Clomiphene citrate | 1 | 1 | |
| Total dose of FSH (IU) | 1650 (1200–2475) | 1275 (150–2250) | 0.0220* |
| Number of oocytes retrieved | 14.5 (2–28) | 8.5 (1–12) | 0.0324* |

Data are median (range) unless stated otherwise.

*Antagonist, Stimulation with FSH, adding GnRH antagonist when at least one follicle reaches 14 mm in diameter; FSH, Stimulation only with FSH; Long, Stimulation with FSH under the suppression of endogenous gonadotrophins by administration of GnRH agonist starting at mid luteal phase of the previous cycle; Clomiphene Citrate: Stimulation only with clomiphene citrate. *P < 0.05.

37 °C for 30 minutes. The suspension was layered over Ficoll-Paque (GE Healthcare, Buckinghamshire, UK) and centrifuged at 700 g for 30 minutes. GLCs were collected from the interface and washed with PBS. GLCs were cultured in 6- or 48-well plates at a density of 2×10^5 cells/mL in Dulbecco's modified Eagle's medium F-12 (DMEM/F12) (Thermo Fisher Scientific, Waltham, MA, USA) containing 10% v/v fetal bovine serum (Sigma-Aldrich) and antibiotics (100 U/mL penicillin, 0.1 mg/mL streptomycin, and 250 ng/mL amphotericin B; Sigma-Aldrich). All GLCs were precultured for 3–5 days prior to treatment at 37 °C in a humidified atmosphere containing 5% CO₂.

Treatment of human GLCs

To evaluate the effect of ER stress on activation of AHR, ARNT, and CYP1B1, human GLCs were pre-incubated for 3–24 hours with ER stress inducers: 2.5 µg/mL tunicamycin (Wako, Osaka, Japan) or 1 µM thapsigargin (Sigma-Aldrich); these conditions were chosen on the basis of previous studies using human granulosa cells (Takahashi *et al.*, 2016, 2017a, b). Based on the results of time-course experiments, in subsequent experiments cells were incubated with tunicamycin for 24 hours. For knockdown of AHR, small interfering RNAs (siRNAs) were obtained from Dharmacon (GE Healthcare) as SMART pools: ON-TARGETplus human AHR siRNA (L-004990-00-0020) for knockdown and ON-TARGETplus non-targeting pool (D-001810-10-20) as the negative control. GLCs were transfected with 10 nM siRNA for 24 hours in Opti-MEM reduced-serum medium (Thermo Fisher Scientific) using Lipofectamine RNAiMAX (Thermo Fisher Scientific). After transfection, the medium was removed, and GLCs were treated with tunicamycin for 24 hours.

RNA extraction, reverse transcription, and real-time quantitative PCR

cDNA templates were synthesized from human GLCs using the SuperPrep Cell Lysis & RT kit for qPCR (TOYOBO, Osaka, Japan).

To quantitate mRNA levels of AHR, ARNT, and CYP1B1, real-time PCR was performed on a Light Cycler system (Roche Diagnostics GmbH, Mannheim, Germany). Human GAPDH mRNA was used as an internal standard for RNA loading. Primer sequences were as follows: human AHR (sense, 5'-AGAGTTGGACCGTTTGGCTA-3'; antisense, 5'-AGTTATCCTGGCCTCCGTTT-3'), human ARNT (sense, 5'-CAAGCCCCTTGAGAAGTCAG-3'; antisense, 5'-GGGGTAGGAGGGAATGTGTT-3'), human CYP1B1 (sense, 5'-AAGTTCTTGAGGC ACTGCGAA-3'; antisense, 5'-GGCCGGTACGTTCTCCAAAT-3'), and human GAPDH (sense, 5'-TGGACCTGACCTGCCGTCTA-3'; antisense, 5'-CTGCTTACCACCTTCTTGA-3'). PCR conditions were as follows: 40 cycles of 98 °C for 10 seconds, 60 °C for 10 seconds, and 68 °C for 30 seconds. All samples from GLCs were analyzed in quadruplicate.

Western blot analysis

Human GLCs were cultured in 6-well culture plates. After stimulation, the GLCs were lysed in lysis buffer (Merck, Darmstadt, Germany) and centrifuged at 1430 g for 10 minutes at 4 °C to remove insoluble material. The supernatants were collected, and the protein concentration was measured using the Bio-Rad Protein Assay (Bio-Rad Laboratories, Hercules, CA, USA). Extracted proteins (20 µg/lane for AHR, 10 µg/lane for CYP1B1) were resolved on Any kD and 10% Mini-PROTEAN TGX Precast Protein Gels (Bio-Rad), respectively. After electrophoretic transfer onto Trans-Blot Turbo Transfer Packs (Bio-Rad) using the Trans-Blot Turbo Transfer System (Bio-Rad), membranes were blocked for 1 hour at room temperature with 5% w/v skim milk in Tris-buffered saline containing 0.1% v/v Tween-20 (TBST). The blocked membranes were probed overnight at 4 °C with anti-AHR (RRID: AB_2226163, 1:1000; Proteintech), anti-CYP1B1 (RRID: AB_731810, 1:1000; Abcam), or anti-β-actin antibody (RRID: AB_476697, 1:3000; Sigma-Aldrich). After incubation with secondary

antibody (anti-rabbit RRID: AB_2099233 or anti-mouse RRID: AB_330924 at 1:2000 for AHR, 1:16000 for CYP11B1, and 1:5000 for β -actin; Cell Signaling Technology, Danvers, MA, USA) for 1 hour at room temperature, proteins were visualized using the ECL Plus western blotting detection reagents (GE Healthcare). Images were acquired on an Image Quant LAS 4000 (GE Healthcare). β -actin was used as a loading control. The immunoblot procedure was repeated using five different samples, and all samples were analyzed in triplicate. Quantification of band intensity was performed using the ImageJ software (RRID: SCR_003073, National Institutes of Health) (Schneider et al., 2012).

CYP11B1 activity assay

CYP11B1 activity was determined using the P450-Glo™ CYP11B1 Assay kit (Promega, Madison, WI, USA). Briefly, human GLCs were seeded into 24-well plates, and treated with siAHR and tunicamycin. The medium was replaced with medium containing 100 μ M Luciferin-CEE, and the cells were incubated for 3 hours at 37 °C under 5% CO₂. Fifty microliters of medium was transferred to an opaque white 96-well plate containing 50 μ L luciferin detection reagent, and the plate was incubated for 20 minutes at room temperature. Luminescence was measured with a Synergy LX luminometer (BioTek, Tokyo, Japan). Enzymatic activity was normalized against protein content.

Determination of estrus cycle

A vaginal smear was performed on each mouse every day from day 12 of treatment until the day of sacrifice. Detached vaginal cells were collected by washing the vagina with normal saline. After air drying, the smears were treated with Diff-Quick Solution (Sysmex, Kobe, Japan) and examined by microscopy to determine the stage of the estrus cycle. The stage was determined as previously described (Byers et al., 2012; Ajayi and Akhigbe, 2020). Briefly, the mouse estrus cycle is divided into four phases: proestrus, estrus, metestrus, and diestrus. In proestrus, the smear consisted primarily of nucleated epithelial cells. Smears with predominantly cornified epithelial cells were classified as estrus. Metestrus smears had an equal proportion of leukocytes, cornified, and nucleated epithelial cells. In diestrus, smears consisted mainly of leukocytes.

Histology

Mouse ovaries were fixed in 10% v/v neutral buffered formalin, embedded in paraffin, and sectioned at a thickness of 5 μ m. Sections were stained with hematoxylin and eosin, and the number of atretic antral follicles were counted in every sixth section across the entire ovary as previously described (Azhar et al., 2020). To ensure that each atretic antral follicle was only counted once, adjacent sections were also analyzed. Atretic follicles were identified by the shrinkage or disappearance of granulosa cell walls and cumulus cells, the hyperplasia of theca cells, and the appearance of macrophages in the antrum (Osman, 1985; Kauffman et al., 2015).

Statistical analysis

All statistical analyses were performed using the JMP pro 14 software (RRID: SCR_014242; SAS Institute Inc., Cary, NC, USA). All data are

shown as means \pm SEM. The Student's t-test was used for comparisons between pairs of samples, and the Tukey–Kramer honest significant difference test was used for multiple comparisons. A value of $P < 0.05$ was considered statistically significant.

Results

Expression of AHR, ARNT, and CYP11B1 is elevated in granulosa cells of PCOS patients

To examine the expression of AHR in granulosa cells, we performed immunohistochemical analysis of ovaries from PCOS ($n = 5$) and control ($n = 5$) patients. As shown in Fig. 1a–c, immunoreactivity of AHR was higher in the granulosa cells of ovaries from PCOS patients. For further confirmation of the elevated expression of AHR in the granulosa cells of PCOS patients, we performed quantitative PCR to measure the AHR mRNA level in GLCs from PCOS ($n = 12$) and control ($n = 12$) patients harvested at IVF. The level of AHR mRNA was significantly higher in GLCs from PCOS patients (Fig. 1d). We also measured the expression levels of ARNT, an AHR nuclear translocator protein that forms a complex with AHR, and CYP11B1, a xenobiotic metabolizing enzyme induced by activation of AHR. As shown in Fig. 1e–g and Fig. 1i–k, expression of ARNT and CYP11B1 protein was elevated in the granulosa cells of ovaries from PCOS patients. ARNT and CYP11B1 mRNA levels were also elevated in GLCs of PCOS patients, consistent with the findings for AHR (Fig. 1h and l).

Expression of AHR, ARNT, and CYP11B1 is elevated in granulosa cells of PCOS model mice

We then examined the expression of AHR, ARNT, and CYP11B1 in the ovaries of a PCOS mouse model. As shown in Fig. 2, immunohistochemical analysis revealed that AHR, ARNT, and CYP11B1 protein levels were higher in the granulosa cells of PCOS mice than in those of control mice. These observations in PCOS mice were in accordance with those acquired from human specimens.

ER stress induces AHR, ARNT, and CYP11B1 mRNA expression in cultured human GLCs

To determine whether ER stress activates expression of AHR, ARNT, and CYP11B1 in cultured human GLCs, we measured the levels of AHR, ARNT, and CYP11B1 mRNA following treatment with an ER stress inducer, tunicamycin or thapsigargin. Tunicamycin and thapsigargin induce ER stress in different manners: tunicamycin by blocking N-linked glycosylation, resulting in accumulation of misfolded protein in the ER; and thapsigargin by inhibiting Ca²⁺ uptake into ER, thereby attenuating the organelle's protein-folding capacity. Both tunicamycin and thapsigargin increased the levels of AHR, ARNT, and CYP11B1 mRNA in a time-dependent manner (Fig. 3).

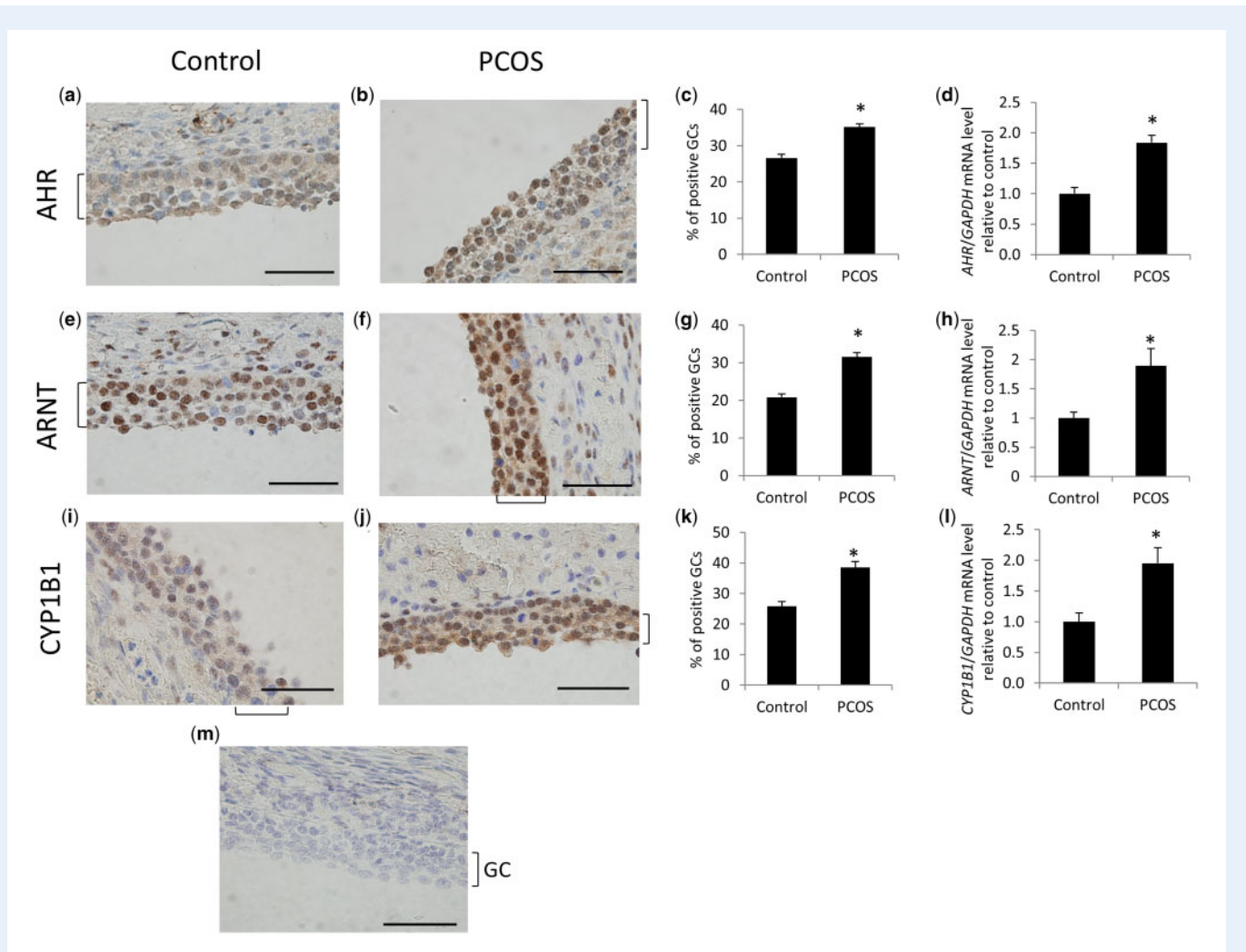


Figure 1 Aryl hydrocarbon receptor (AHR), aryl hydrocarbon receptor nuclear translocator (ARNT), and cytochrome 450 IBI (CYP11B1) are upregulated in granulosa cells of polycystic ovary syndrome (PCOS) ovaries and granulosa-lutein cells (GLCs) from PCOS patients. Immunohistochemistry was performed on ovaries of patients with or without PCOS (a–c, e–g, i–k), and real-time PCR was performed in GLCs from control participants and patients with PCOS (d, h, l). Cross-sections of ovaries of five control patients and five PCOS patients were stained with AHR antibody (a, b), ARNT antibody (e, f), and CYP11B1 antibody (i, j) and counterstained with hematoxylin. Representative sections are shown. (m) Corresponding negative control. The scale bars indicate 50 μ m. (c, g, k) Quantitative analysis of immunohistochemical staining. Values are means \pm SEM. mRNA levels of AHR (d), ARNT (h), and CYP11B1 (l) in GLCs from control participants and patients with PCOS ($n = 12$, respectively) were measured by real-time PCR and normalized against GAPDH mRNA. Values are means \pm SEM, expressed relative to the mean control value. * $P < 0.05$ relative to controls. GC, granulosa cell layers.

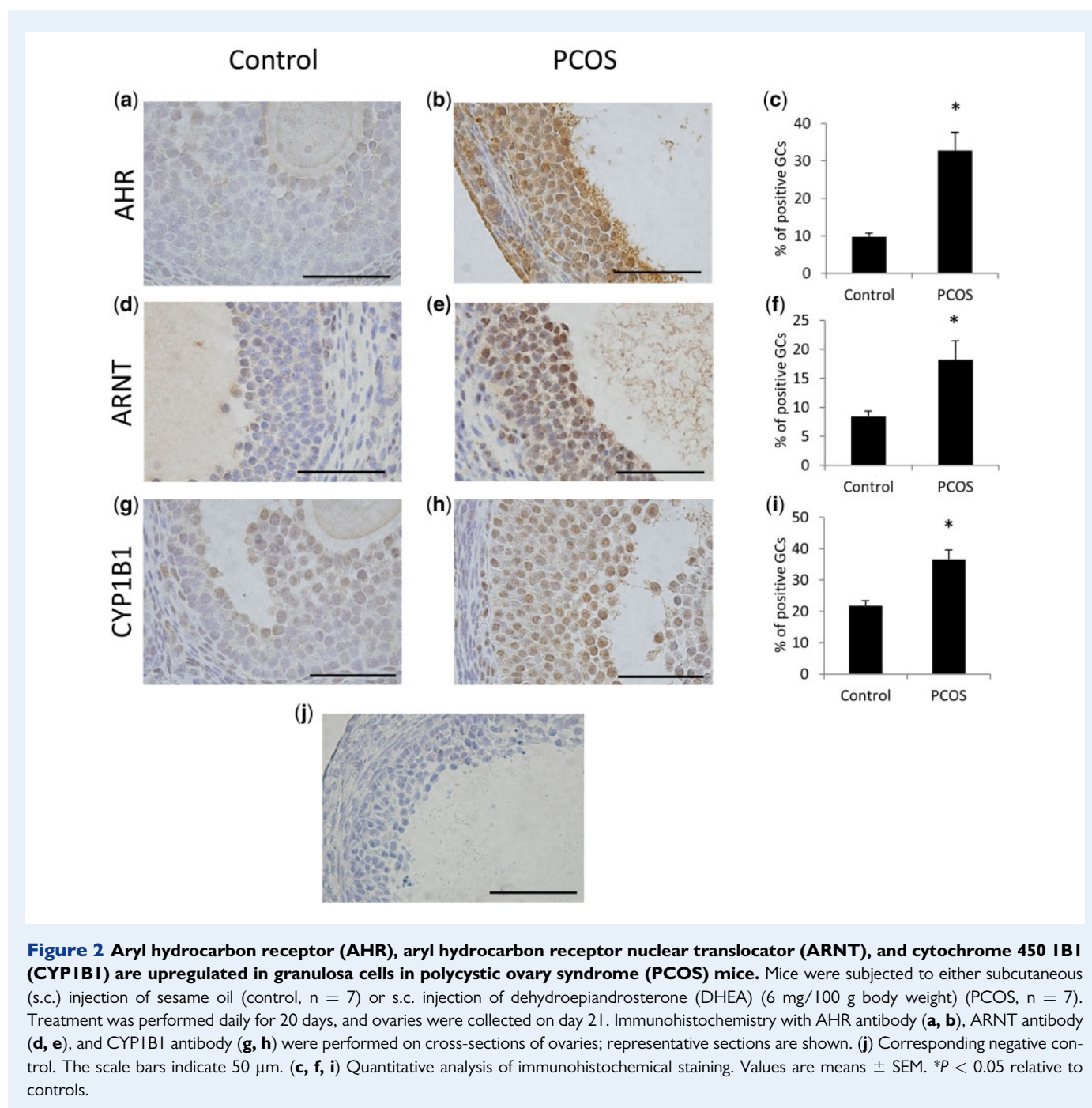
AHR induced by ER stress mediates upregulation of expression and activity of CYP11B1 in cultured human GLCs

We next examined whether AHR is necessary for activation of CYP11B1 in response to ER stress. Based on the results shown in Fig. 3, hereafter we used only tunicamycin as an ER stress inducer. In these experiments, AHR was knocked down by RNA interference, and the cells were then treated with tunicamycin. Pretreatment with siAHR abrogated the tunicamycin-induced increase in CYP11B1 mRNA level, with a concomitant reduction in AHR mRNA (Fig. 4a and b). As shown in Fig. 4c–e, treatment with tunicamycin increased AHR and CYP11B1 protein expression, and this increase was abrogated by knockdown of

AHR. Treatment with tunicamycin increased CYP11B1 activity, and this effect was also abrogated by knockdown of AHR (Fig. 4f). Collectively, these findings showed that ER stress induced expression of AHR, which in turn induced activation of CYP11B1 in cultured GLCs.

Administration of an AHR antagonist restores the estrous cycle and ovarian morphology in mice with PCOS, with a concomitant reduction in AHR and CYP11B1 expression in granulosa cells

To determine whether the AHR–CYP11B1 pathway, which is upregulated in granulosa cells, is involved in the pathophysiology of PCOS, we treated



PCOS model mice with the AHR antagonist CH223191. As shown in Fig. 5a–c, administration of CH223191 restored the estrous cycle of PCOS mice: no cyclicity was observed in PCOS mice, whereas CH223191-treated PCOS mice showed cyclicity. Treatment with CH223191 also restored normal ovarian morphology in PCOS mice, with a significant reduction in the number of atretic follicles (Fig. 5d–g). Treatment of PCOS mice with CH223191 decreased the expression of AHR and CYP11B1 in granulosa cells, indicating that systemic administration of the drug locally downregulated the AHR–CYP11B1 pathway (Fig. 6).

Discussion

The results of this study show that expression of AHR, ARNT, and CYP11B1 was higher in the granulosa cells of PCOS patients and in a mouse model of PCOS than in the corresponding controls. ER stress in human GLCs upregulated AHR and ARNT, which in turn increased the expression and activity of CYP11B1. Administration of the AHR antagonist CH223191 to PCOS mice restored estrous cycling and decreased the number of atretic follicles, concomitant with a reduction in expression of AHR and CYP11B1 in granulosa cells.

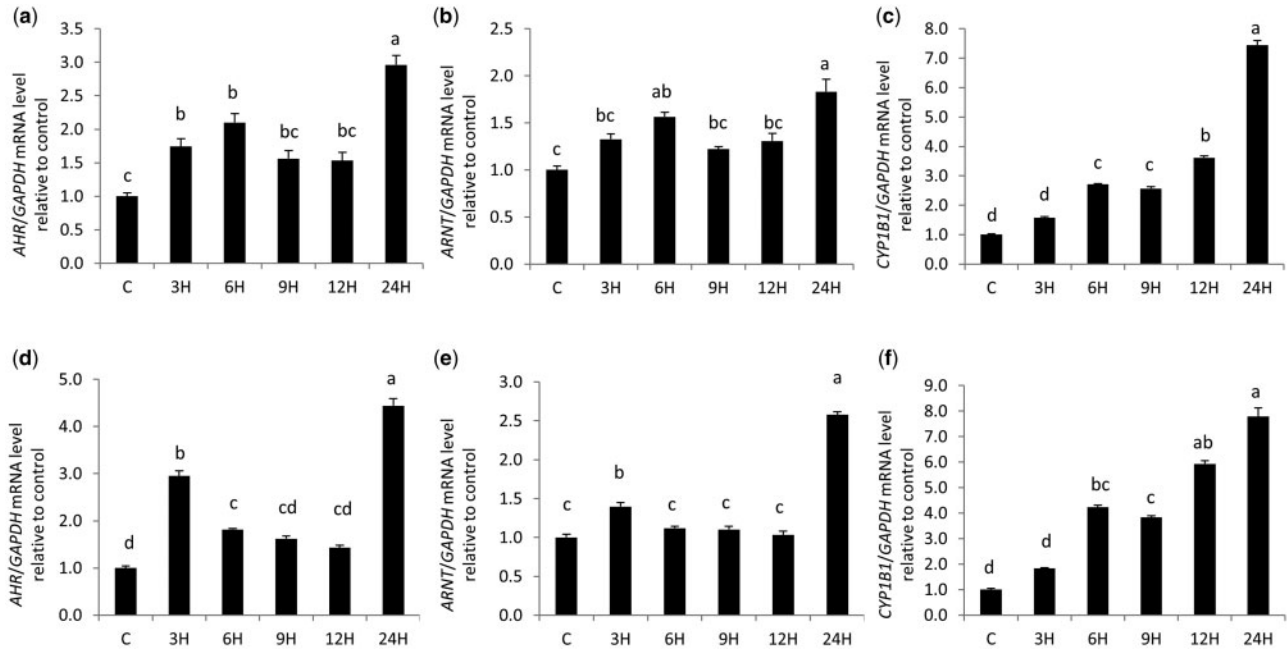


Figure 3 Effects of endoplasmic reticulum (ER) stress on aryl hydrocarbon receptor (AHR), aryl hydrocarbon receptor nuclear translocator (ARNT), and cytochrome 450 1B1 (CYP1B1) mRNA levels in cultured human granulosa-lutein cells (GLCs). Human GLCs were pre-incubated with an ER stress inducer, 2.5 µg/mL tunicamycin (a–c) or 1 µM thapsigargin (d–f) for 3–24 hours. Levels of AHR (a, d), ARNT (b, e), and CYP1B1 mRNA (c, f) in GLCs were measured by quantitative PCR. Data were normalized against the corresponding levels of GAPDH mRNA. Values are means ± SEM in quadruplicate samples, expressed relative to the control. Representative data are shown, and at least three replicate experiments were performed on three different samples. Letters denote significant differences between groups.

Expression of AHR was upregulated, and its downstream signaling was activated, in the granulosa cells of PCOS patients. In addition, administration of an AHR antagonist to a PCOS mouse model improved the reproductive phenotype of PCOS. To characterize the activation of AHR downstream signaling, we evaluated the expression and activity of CYP1B1, which is expressed abundantly in human ovary in a manner that is correlated with AHR activity (Hao *et al.*, 2012; Fagerberg *et al.*, 2014; Stockinger *et al.*, 2014). AHR was originally identified as a receptor for several EDCs, including polychlorinated dibenzodioxins (commonly referred to as dioxins), polychlorinated biphenyls (PCBs), and polycyclic aromatic hydrocarbons (PAHs). The canonical AHR–ARNT–CYP1B1 pathway is activated upon binding of EDCs to AHR. Upon interaction with a ligand, AHR translocates from the cytoplasm to the nucleus and dimerizes with its partner ARNT. The AHR/ARNT heterodimer binds to xenobiotic response elements (XREs), activating AHR target genes including those involved in xenobiotic metabolism (Swedenborg *et al.*, 2009). EDCs are intimately involved in PCOS pathology: serum levels of AHR ligands, including PCBs and PAHs, are higher in PCOS patients than in control patients, and exposure to cigarette smoke, the source of PAHs, is associated with aggravated hormonal and metabolic profiles in PCOS patients (Cupisti *et al.*, 2010; Vagi *et al.*, 2014; Yang *et al.*, 2015; Rutkowski and Diamanti-Kandarakis, 2016; Xirofotou *et al.*, 2016; Li *et al.*, 2018). These findings, together with the novel role of AHR independent of its activity as an EDC receptor, prompted us to explore the role of AHR

itself in the pathology of PCOS. Although previous research focused on AHR-mediated toxicology, more recent studies identified a large number of endogenous and phytochemical AHR ligands and highlighted the role of AHR and its associated pathways in multiple metabolic and pathologic processes, including obesity, nonalcoholic fatty liver disease, atopic dermatitis, and cancer progression, independently of its activity as an EDC receptor (Murray *et al.*, 2014; Esser *et al.*, 2018; Bock, 2020). Our findings that the AHR pathway is activated in granulosa cells of PCOS and that inhibition of AHR improves the phenotype suggest that AHR plays a crucial role in the pathology of PCOS.

ER stress increased the expression of AHR, ARNT, and CYP1B1 in human cultured GLCs, and knockdown of AHR abrogated the ER stress-induced upregulation and activation of CYP1B1, suggesting that ER stress induces AHR expression and activates downstream signaling. Recent studies revealed that various stimuli, including growth factors and hormones, can modulate expression and activation of AHR even in the absence of its ligands (Harper *et al.*, 2006; Larigot *et al.*, 2018). Intriguingly, AHR is ubiquitously expressed in multiple tissues, and the mechanisms regulating its expression and activation differ among cell types. For example, transforming growth factor (TGF)-β decreases AHR expression in a lung carcinoma cell line, but has no effect in rat granulosa cells or in a breast cancer cell line (Bussmann and Baraño, 2008). Only a few studies have examined the mechanisms regulating AHR expression in granulosa cells in the absence of exogenous ligands. Treatment of cultured granulosa cells with FSH or 17β-estradiol (E2)

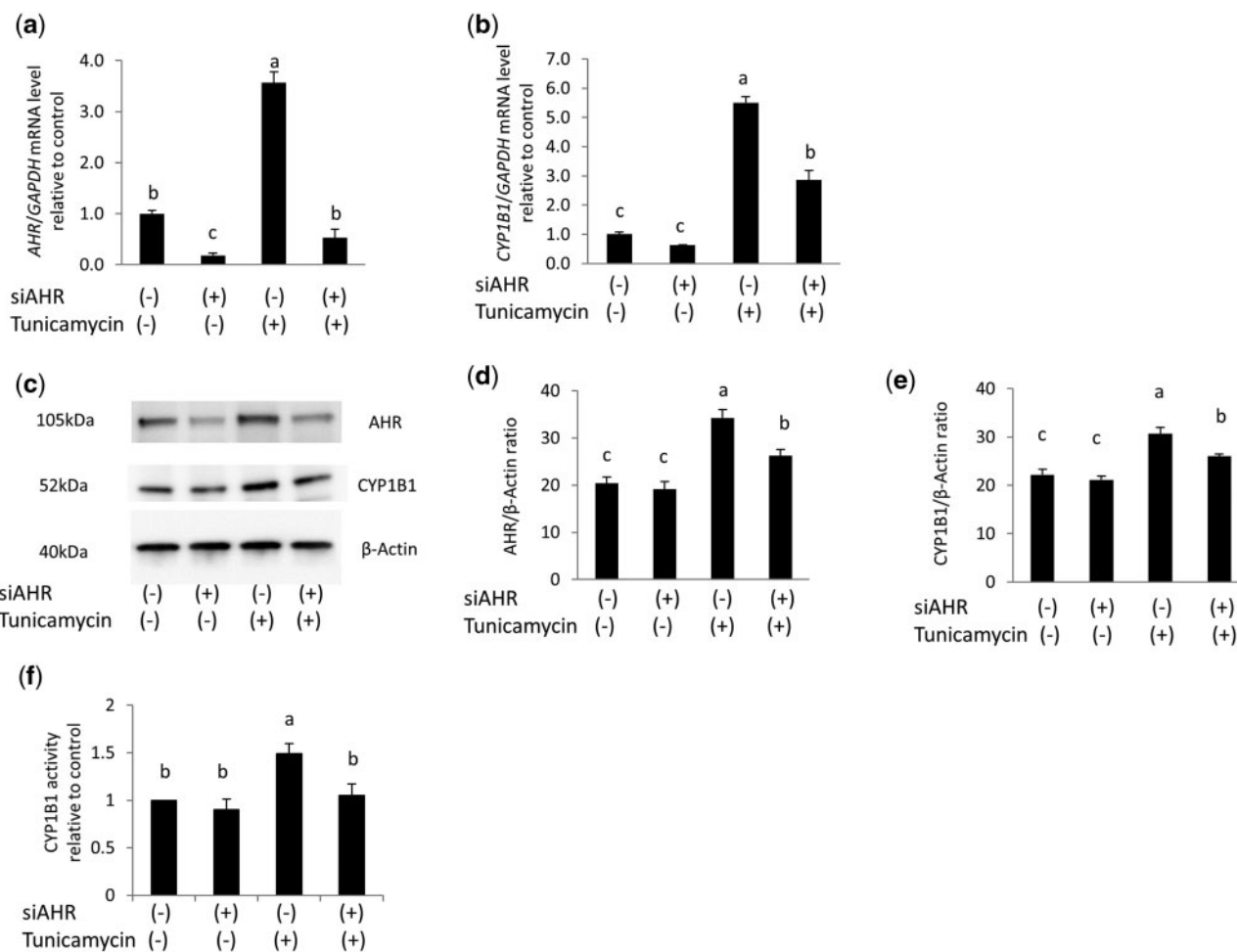


Figure 4 Aryl hydrocarbon receptor (AHR) mediates endoplasmic reticulum (ER) stress-induced upregulation of cytochrome 450 1B1 (CYP1B1) mRNA, protein, and activity in cultured human granulosa-lutein cells (GLCs). Human GLCs were transfected with AHR siRNA (10 nM) or negative control (10 nM), followed by incubation for 24 hours with 2.5 μ g/mL tunicamycin, an ER stress inhibitor. AHR (a) and CYP1B1 mRNA levels (b) in GLCs were examined by quantitative PCR. Data were normalized against the corresponding levels of GAPDH mRNA. Values are shown as means \pm SEM in quadruplicate samples, expressed relative to the control. Representative data are shown, and at least three replicate experiments were performed on three different samples. (c–e) Western blot analysis was performed with anti-AHR or anti-CYP1B1 antibodies. β -Actin was used as a loading control. (c) Representative data are shown, and at least five replicate experiments were performed on five different samples. (d, e) The results of quantitative analysis are shown as means \pm SEM. (f) CYP1B1 activity assay. All samples from GLCs were analyzed in sextuplicate. Values are means \pm SEM, expressed relative to the mean control value. Letters denote significant differences between groups.

decreases expression of AHR mRNA and protein (Bussmann and Baraño, 2006). *In vivo* administration of pregnant mare serum gonadotropin (PMSG) to immature mice increases the *Ahr* mRNA level in granulosa cells, whereas subsequent human chorionic gonadotropin (hCG) treatment decreases it; these effects are controlled at the level of transcription rate (Teino et al., 2014; Matvere et al., 2019). Given that promoter lesions of AHR harbor multiple binding sites for C/EBP homologous protein (CHOP), a UPR factor induced by ER stress, it is conceivable that ER stress regulates AHR expression at the transcription level. Notably in this regard, testosterone exerts stimulatory effects on the AHR system in granulosa cells, similar to the effects of ER stress reported here; specifically, it induces expression of AHR and ARNT at the mRNA

and protein levels, thereby activating downstream signaling of AHR (Wu et al., 2013). Recent studies showed that ER stress is activated in granulosa cells of PCOS patients, modulates various cellular functions, and contributes to PCOS pathology (Takahashi et al., 2017a; Azhary et al., 2019; 2020; Jin et al., 2020). Interestingly, it was also showed that ER stress is activated by testosterone in granulosa cells (Azhary et al., 2019; Jin et al., 2020). Hyperandrogenism and ER stress in the follicular microenvironment in PCOS may cooperatively contribute to induction of AHR and activation of its downstream pathway.

In this study, administration of the AHR antagonist CH223191 to PCOS mice restored estrous cycling and decreased the number of atretic antral follicles, with a concomitant reduction in expression of AHR and CYP1B1 protein in granulosa cells. This suggests that

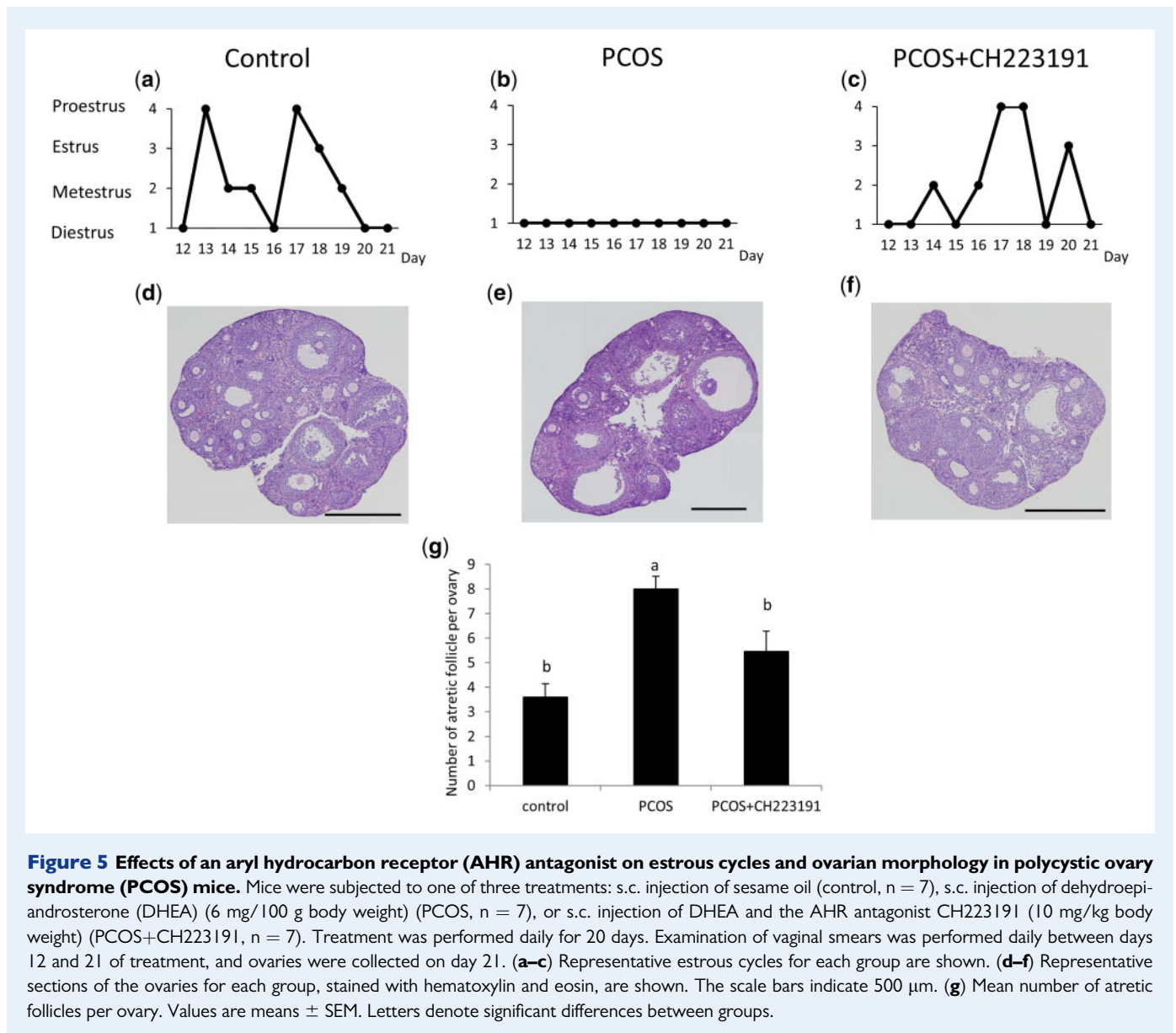
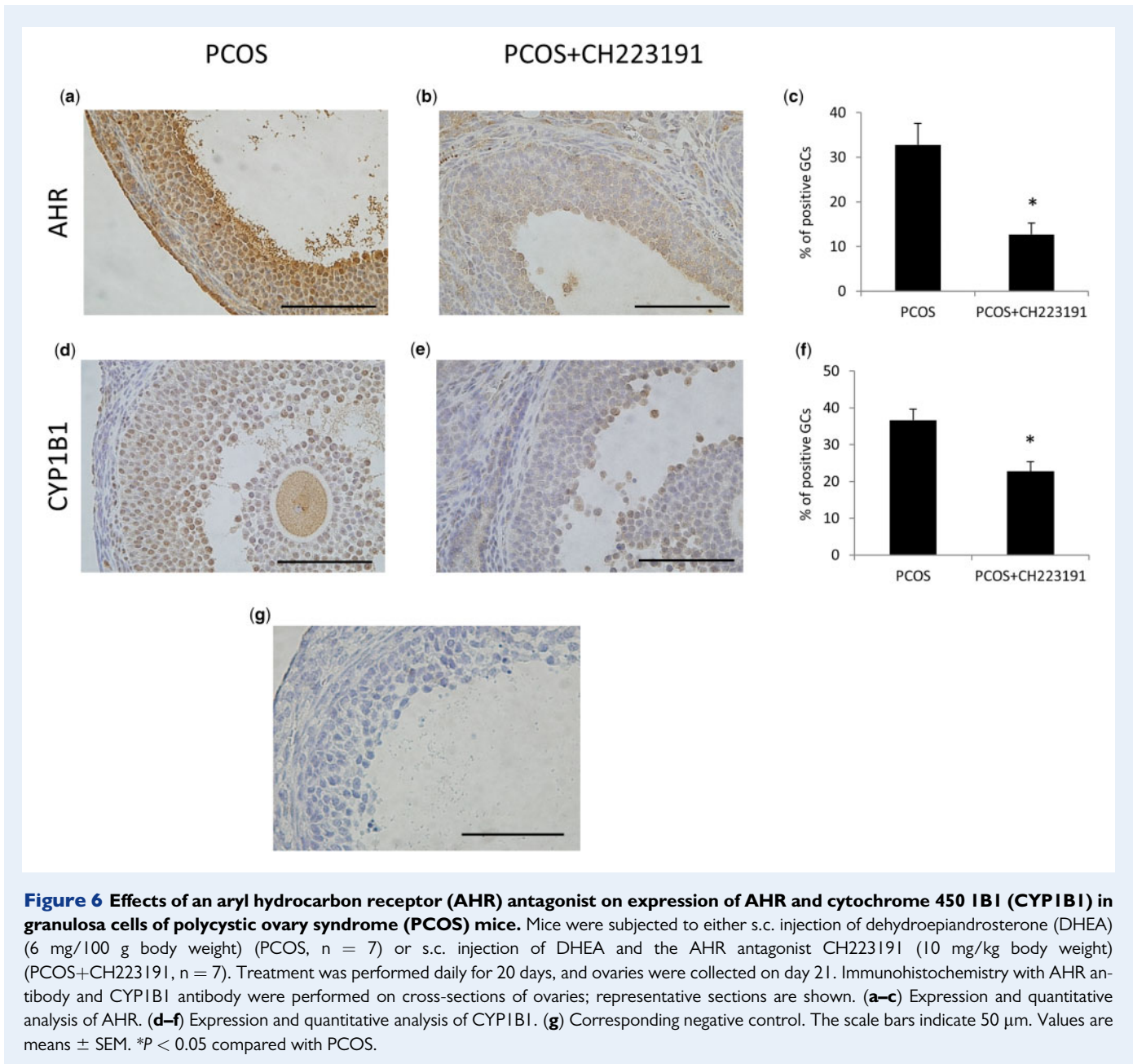


Figure 5 Effects of an aryl hydrocarbon receptor (AHR) antagonist on estrous cycles and ovarian morphology in polycystic ovary syndrome (PCOS) mice. Mice were subjected to one of three treatments: s.c. injection of sesame oil (control, $n = 7$), s.c. injection of dehydroepiandrosterone (DHEA) (6 mg/100 g body weight) (PCOS, $n = 7$), or s.c. injection of DHEA and the AHR antagonist CH223191 (10 mg/kg body weight) (PCOS+CH223191, $n = 7$). Treatment was performed daily for 20 days. Examination of vaginal smears was performed daily between days 12 and 21 of treatment, and ovaries were collected on day 21. (a–c) Representative estrous cycles for each group are shown. (d–f) Representative sections of the ovaries for each group, stained with hematoxylin and eosin, are shown. The scale bars indicate 500 μm . (g) Mean number of atretic follicles per ovary. Values are means \pm SEM. Letters denote significant differences between groups.

systemic administration of CH223191 effectively attenuates local activation of the AHR system in the ovary, and that inhibition of AHR represents a novel therapeutic approach in PCOS. It remains to be determined how overexpression of AHR and activation of downstream signaling in granulosa cells contributes to PCOS pathology. It is conceivable that activation of CYP11B1 plays a role in this process. The high levels of CYP11B1 in granulosa cells of PCOS detected in this study were consistent with previous findings that *CYP11B1* mRNA expression is higher in cumulus cells harvested from PCOS patients than in those from non-PCOS patients (Haouzi *et al.*, 2012). Given that CYP11B1 is involved in the metabolism of E2, low levels of E2 in serum or follicular fluid in PCOS patients are partly attributable to the elevated expression and activation of CYP11B1 in granulosa cells (Henríquez *et al.*, 2020; Jarrett *et al.*, 2020). Interestingly, *CYP11B1* mRNA expression is also upregulated in adipose tissue of PCOS patients (Kokosar *et al.*, 2016). In this study, we examined CYP11B1 as a representative AHR

target gene because the best-characterized AHR function to date is protection against xenobiotics through induction of CYPs. However, recent studies showed that AHR also interacts with multiple cellular pathways and gene sets in several pathological conditions closely related to PCOS, such as obesity and inflammation (Esser *et al.*, 2018; Larigot *et al.*, 2018; Guarnieri *et al.*, 2020). Activation of AHR plays a key role in adiposity and liver steatosis in high-fat diet-induced obese mice by inducing CYP11B1, peroxisome proliferator-activated receptor γ (PPAR γ) target genes such as fibroblast growth factor 21 (FGF21), and stearoyl-CoA desaturase 1 (SCD1) in the liver (Moyer *et al.*, 2017; Girer *et al.*, 2019; Rojas *et al.*, 2020). AHR also participates in immune system regulation and inflammation. The inflammatory cytokine interleukin-6 (IL-6) and AHR are involved in an autoinflammatory loop: IL-6 increases expression and activation of AHR, and activated AHR in turn activates transcription of IL-6 (Guarnieri *et al.*, 2020). Future studies should seek to uncover the diverse roles of AHR



activation in granulosa cells in PCOS pathogenesis. It will also be necessary to elucidate whether AHR signaling in granulosa cells or outside the ovary contributes to the metabolic phenotype of PCOS. We did not address this question in this study because the DHEA-induced model that we used provides information about the genesis of ovarian abnormalities, but the animals do not develop obesity and the metabolic dysfunction is not completely phenotyped (Maliqueo et al., 2014; Osuka et al., 2019).

In summary, AHR expression and downstream signaling are activated in granulosa cells from PCOS ovaries, and these changes are induced by ER stress. Moreover, downregulation of local AHR expression and activation restores a normal reproductive phenotype in a PCOS mouse model. Our findings show that AHR activated by ER

stress in the follicular microenvironment contributes to PCOS pathology. Thus, AHR represents a novel therapeutic target for PCOS.

Data availability

The authors confirm that the data supporting the findings of this study are available within the article.

Acknowledgments

The authors thank Dr. Kazunori Matsumoto from Matsumoto Ladies' Clinic, Dr. Xiaohui Tang from Akihabara ART Clinic, and Dr. Toshihiro

Fujiwara from Phoenix ART Clinic for providing the human samples. We also thank Nagisa Oi from the University of Tokyo Hospital for technical assistance.

Authors' roles

C.K. designed and performed experiments, analyzed, and interpreted data, and wrote the article. M.H. contributed to conception of the work, analyzed and interpreted data, and wrote the article. A.K., J.M.K.A., E.N., H.K., and Z.X. performed experiments. Y.U., N.T., O.W.-H., Y.H., K.K., T.F., and Y.O. contributed to study design, data interpretation, and article revision.

Funding

This study was supported by Grants-in-Aid for Scientific Research from the Japan Society for the Promotion of Science (JSPS) (grant number 19k09749 to M.H.), (grant number 19k24021 to N.T.), (grant number 19k24045 to Y.U.), and a grant from the Takeda Science Foundation (to M.H.).

Conflict of interest

The authors declare no conflict of interest.

References

- Ajayi AF, Akhigbe RE. Staging of the estrous cycle and induction of estrus in experimental rodents: an update. *Fertil Res Pract* 2020;**6**: 5.
- Azhary JMK, Harada M, Takahashi N, Nose E, Kunitomi C, Koike H, Hirata T, Hirota Y, Koga K, Wada-Hiraike O et al. Endoplasmic reticulum stress activated by androgen enhances apoptosis of granulosa cells via induction of death receptor 5 in PCOS. *Endocrinology* 2019;**160**:119–132.
- Azhary JMK, Harada M, Kunitomi C, Kusamoto A, Takahashi N, Nose E, Oi N, Wada-Hiraike O, Urata Y, Hirata T et al. Androgens increase accumulation of advanced glycation end products in granulosa cells by activating ER stress in PCOS. *Endocrinology* 2020;**161**:1–13.
- Bock KW. Aryl hydrocarbon receptor (AHR) functions: balancing opposing processes including inflammatory reactions. *Biochem Pharmacol* 2020;**178**:114093.
- Bussmann UA, Barañao JL. Regulation of aryl hydrocarbon receptor expression in rat granulosa cells. *Biol Reprod* 2006;**75**:360–369.
- Bussmann UA, Barañao JL. Interaction between the aryl hydrocarbon receptor and transforming growth factor-beta signaling pathways: evidence of an asymmetrical relationship in rat granulosa cells. *Biochem Pharmacol* 2008;**76**:1165–1174.
- Byers SL, Wiles MV, Dunn SL, Taft RA. Mouse estrous cycle identification tool and images. *PLoS One* 2012;**7**:e35538.
- Cupisti S, Häberle L, Dittrich R, Oppelt PG, Reissmann C, Kronawitter D, Beckmann MW, Mueller A. Smoking is associated with increased free testosterone and fasting insulin levels in women with polycystic ovary syndrome, resulting in aggravated insulin resistance. *Fertil Steril* 2010;**94**:673–677.
- Dean A, Gregorc T, Docherty CK, Harvey KY, Nilsen M, Morrell NW, MacLean MR. Role of the aryl hydrocarbon receptor in sugen 5416-induced experimental pulmonary hypertension. *Am J Respir Cell Mol Biol* 2018;**58**:320–330.
- Elia E, Sander V, Luchetti CG, Solano ME, Di Girolamo G, Gonzalez C, Motta AB. The mechanisms involved in the action of metformin in regulating ovarian function in hyperandrogenized mice. *Mol Hum Reprod* 2006;**12**:475–481.
- Escobar-Morreale HF. Polycystic ovary syndrome: definition, aetiology, diagnosis and treatment. *Nat Rev Endocrinol* 2018;**14**: 270–284.
- Esser C, Lawrence BP, Sherr DH, Perdew GH, Puga A, Barouki R, Coumoul X. Old receptor, new tricks—the ever-expanding universe of aryl hydrocarbon receptor functions. Report from the 4th AHR Meeting, 29–31 August 2018 in Paris, France. *IJMS* 2018;**19**:3603.
- Fagerberg L, Hallström BM, Oksvold P, Kampf C, Djureinovic D, Odeberg J, Habuka M, Tahmasebpoor S, Danielsson A, Edlund K et al. Analysis of the human tissue-specific expression by genome-wide integration of transcriptomics and antibody-based proteomics. *Mol Cell Proteomics* 2014;**13**:397–406.
- Girer NG, Carter D, Bhattarai N, Mustafa M, Denner L, Porter C, Elferink CJ. Inducible loss of the aryl hydrocarbon receptor activates perigonadal white fat respiration and brown fat thermogenesis via fibroblast growth factor 21. *IJMS* 2019;**20**:950.
- Guarnieri T, Abruzzo PM, Bolotta A. More than a cell biosensor: aryl hydrocarbon receptor at the intersection of physiology and inflammation. *Am J Physiol Cell Physiol* 2020;**318**:C1078–C1082.
- Hao N, Lee KL, Furness SG, Bosdotter C, Poellinger L, Whitelaw ML. Xenobiotics and loss of cell adhesion drive distinct transcriptional outcomes by aryl hydrocarbon receptor signaling. *Mol Pharmacol* 2012;**82**:1082–1093.
- Haouzi D, Assou S, Monzo C, Vincens C, Dechaud H, Hamamah S. Altered gene expression profile in cumulus cells of mature MII oocytes from patients with polycystic ovary syndrome. *Hum Reprod* 2012;**27**:3523–3530.
- Harper PA, Riddick DS, Okey AB. Regulating the regulator: factors that control levels and activity of the aryl hydrocarbon receptor. *Biochem Pharmacol* 2006;**72**:267–279.
- Henríquez S, Kohen P, Xu X, Villarroel C, Muñoz A, Godoy A, Strauss JF, Devoto L. Significance of pro-angiogenic estrogen metabolites in normal follicular development and follicular growth arrest in polycystic ovary syndrome. *Hum Reprod* 2020;**35**: 1655–1665.
- Hetz C, Zhang K, Kaufman RJ. Mechanisms, regulation and functions of the unfolded protein response. *Nat Rev Mol Cell Biol* 2020;**21**: 421–438.
- Jarrett BY, Vanden Brink H, Oldfield AL, Lujan ME. Ultrasound characterization of disordered antral follicle development in women with polycystic ovary syndrome. *J Clin Endocrinol Metab* 2020;**105**: 1–15.
- Jin J, Ma Y, Tong X, Yang W, Dai Y, Pan Y, Ren P, Liu L, Fan HY, Zhang Y et al. Metformin inhibits testosterone-induced

- endoplasmic reticulum stress in ovarian granulosa cells via inactivation of p38 MAPK. *Hum Reprod* 2020;**35**:1145–1158.
- Kauffman AS, Thackray VG, Ryan GE, Tolson KP, Glidewell-Kenney CA, Semaan SJ, Poling MC, Iwata N, Breen KM, Duleba AJ et al. A novel letrozole model recapitulates both the reproductive and metabolic phenotypes of polycystic ovary syndrome in female mice. *Biol Reprod* 2015;**93**:69.
- Kokosar M, Benrick A, Perfilyev A, Fornes R, Nilsson E, Maliqueo M, Behre CJ, Sazonova A, Ohlsson C, Ling C et al. Epigenetic and transcriptional alterations in human adipose tissue of polycystic ovary syndrome. *Sci Rep* 2016;**6**:22883.
- Kunitomi C, Harada M, Takahashi N, Azhary JMK, Kusamoto A, Nose E, Oi N, Takeuchi A, Wada-Hiraike O, Hirata T et al. Activation of endoplasmic reticulum stress mediates oxidative stress-induced apoptosis of granulosa cells in ovaries affected by endometrioma. *Mol Hum Reprod* 2020;**26**:40–52.
- Lai H, Jia X, Yu Q, Zhang C, Qiao J, Guan Y, Kang J. High-fat diet induces significant metabolic disorders in a mouse model of polycystic ovary syndrome. *Biol Reprod* 2014;**91**.
- Larigot L, Juricek L, Dairou J, Coumoul X. AhR signaling pathways and regulatory functions. *Biochim Open* 2018;**7**:1–9.
- Li J, Wu Q, Wu XK, Zhou ZM, Fu P, Chen XH, Yan Y, Wang X, Yang ZW, Li WL, for PCOSAct Study Group et al. Effect of exposure to second-hand smoke from husbands on biochemical hyperandrogenism, metabolic syndrome and conception rates in women with polycystic ovary syndrome undergoing ovulation induction. *Hum Reprod* 2018;**33**:617–625.
- Maliqueo M, Benrick A, Stener-Victorin E. Rodent models of polycystic ovary syndrome: phenotypic presentation, pathophysiology, and the effects of different interventions. *Semin Reprod Med* 2014;**32**:183–193.
- Matvere A, Teino I, Varik I, Kuuse S, Tiido T, Kristjuhan A, Maimets T. FSH/LH-dependent upregulation of Ahr in murine granulosa cells is controlled by PKA signaling and involves epigenetic regulation. *IJMS* 2019;**20**:3068.
- Moyer BJ, Rojas IY, Kerley-Hamilton JS, Nemani KV, Trask HW, Ringelberg CS, Gimi B, Demidenko E, Tomlinson CR. Obesity and fatty liver are prevented by inhibition of the aryl hydrocarbon receptor in both female and male mice. *Nutr Res* 2017;**44**:38–50.
- Murray IA, Patterson AD, Perdew GH. Aryl hydrocarbon receptor ligands in cancer: friend and foe. *Nat Rev Cancer* 2014;**14**:801–814.
- Osman P. Rate and course of atresia during follicular development in the adult cyclic rat. *J Reprod Fertil* 1985;**73**:261–270.
- Osuka S, Nakanishi N, Murase T, Nakamura T, Goto M, Iwase A, Kikkawa F. Animal models of polycystic ovary syndrome: A review of hormone-induced rodent models focused on hypothalamus-pituitary-ovary axis and neuropeptides. *Reprod Med Biol* 2019;**18**:151–160.
- Pocar P, Fischer B, Klonisch T, Hombach-Klonisch S. Molecular interactions of the aryl hydrocarbon receptor and its biological and toxicological relevance for reproduction. *Reproduction* 2005;**129**:379–389.
- Rojas IY, Moyer BJ, Ringelberg CS, Tomlinson CR. Reversal of obesity and liver steatosis in mice via inhibition of aryl hydrocarbon receptor and altered gene expression of CYP1B1, PPAR α , SCD1, and osteopontin. *Int J Obes* 2020;**44**:948–963.
- Rotterdam ESHRE/ASRM-Sponsored PCOS consensus workshop group Revised 2003 consensus on diagnostic criteria and long-term health risks related to polycystic ovary syndrome (PCOS). *Hum Reprod* 2004;**19**:41–47.
- Rutkowska AZ, Diamanti-Kandarakis E. Polycystic ovary syndrome and environmental toxins. *Fertil Steril* 2016;**106**:948–958.
- Rutkowski DT, Kaufman RJ. That which does not kill me makes me stronger: adapting to chronic ER stress. *Trends Biochem Sci* 2007;**32**:469–476.
- Schneider CA, Rasband WS, Eliceiri KW. NIH Image to ImageJ: 25 years of image analysis. *Nat Methods* 2012;**9**:671–675.
- Stockinger B, Di Meglio P, Gialitakis M, Duarte JH. The aryl hydrocarbon receptor: multitasking in the immune system. *Annu Rev Immunol* 2014;**32**:403–432.
- Swedenborg E, Rüegg J, Mäkelä S, Pongratz I. Endocrine disruptive chemicals: mechanisms of action and involvement in metabolic disorders. *J Mol Endocrinol* 2009;**43**:1–10.
- Takahashi N, Harada M, Hirota Y, Zhao L, Yoshino O, Urata Y, Izumi G, Takamura M, Hirata T, Koga K et al. A potential role of endoplasmic reticulum stress in development of ovarian hyperstimulation syndrome. *Mol Cell Endocrinol* 2016;**428**:161–169.
- Takahashi N, Harada M, Hirota Y, Nose E, Azhary JM, Koike H, Kunitomi C, Yoshino O, Izumi G, Hirata T et al. Activation of endoplasmic reticulum stress in granulosa cells from patients with polycystic ovary syndrome contributes to ovarian fibrosis. *Sci Rep* 2017a;**7**:10824.
- Takahashi N, Harada M, Hirota Y, Zhao L, Azhary JM, Yoshino O, Izumi G, Hirata T, Koga K, Wada-Hiraike O et al. A potential role for endoplasmic reticulum stress in progesterone deficiency in obese women. *Endocrinology* 2017b;**158**:en.2016-1511–97.
- Takahashi N, Harada M, Azhary JMK, Kunitomi C, Nose E, Terao H, Koike H, Wada-Hiraike O, Hirata T, Hirota Y et al. Accumulation of advanced glycation end products in follicles is associated with poor oocyte developmental competence. *Mol Hum Reprod* 2019;**25**:684–694.
- Teino I, Matvere A, Kuuse S, Ingerpuu S, Maimets T, Kristjuhan A, Tiido T. Transcriptional repression of the Ahr gene by LHCGR signaling in preovulatory granulosa cells is controlled by chromatin accessibility. *Mol Cell Endocrinol* 2014;**382**:292–301.
- Vagi SJ, Azziz-Baumgartner E, Sjödin A, Calafat AM, Dumesic D, Gonzalez L, Kato K, Silva MJ, Ye X, Azziz R. Exploring the potential association between brominated diphenyl ethers, polychlorinated biphenyls, organochlorine pesticides, perfluorinated compounds, phthalates, and bisphenol A in polycystic ovary syndrome: a case-control study. *BMC Endocr Disord* 2014;**14**:86.
- Walter P, Ron D. The unfolded protein response: from stress pathway to homeostatic regulation. *Science* 2011;**334**:1081–1086.
- Wang K, Lv Q, Miao YM, Qiao SM, Dai Y, Wei ZF. Cardamonin, a natural flavone, alleviates inflammatory bowel disease by the inhibition of NLRP3 inflammasome activation via an AhR/Nrf2/NQO1 pathway. *Biochem Pharmacol* 2018;**155**:494–509.
- Wu Y, Baumgarten SC, Zhou P, Stocco C. Testosterone-dependent interaction between androgen receptor and aryl hydrocarbon receptor induces liver receptor homolog 1 expression in rat granulosa cells. *Mol Cell Biol* 2013;**33**:2817–2828.

- Xirofotos D, Trakakis E, Peppas M, Chrelias C, Panagopoulos P, Christodoulaki C, Sioutis D, Kassanos D. The amount and duration of smoking is associated with aggravation of hormone and biochemical profile in women with PCOS. *Gynecol Endocrinol* 2016;**32**:143–146.
- Yang Q, Zhao Y, Qiu X, Zhang C, Li R, Qiao J. Association of serum levels of typical organic pollutants with polycystic ovary syndrome (PCOS): a case-control study. *Hum Reprod* 2015;**30**:1964–1973.